SIAM J. SCI. COMPUT.
Vol. 0, No. 0, pp. 000–000

NUMERICAL SOLUTION OF A REGULARIZED WEIGHTED MEAN CURVATURE FLOW PROBLEM FOR ELECTRICAL CONDUCTIVITY IMAGING*

ALEXANDRE TIMONOV†

Abstract. We propose a new approach to the numerical solution of a coupled physics inverse conductivity problem underlying current density impedance imaging (CDII), which is one of the coupled physics electrical conductivity imaging modalities which has emerged recently in medical diagnostics. The approach is based on a regularized weighted mean curvature flow problem, which is considered to be a novel mathematical model of CDII. It is an alternative to an existing model based on the weighted least gradient problem relative to the Dirichlet condition. A numerical study is performed to demonstrate the consistency and computational feasibility of the regularized weighted mean curvature model presented.

Key words. electrical conductivity imaging, regularized weighted mean curvature, Rothe's method

AMS subject classifications. 35K55, 35K65, 35K93, 65L09, 65L12, 65N20, 65N40

DOI. 10.1137/18M1236071

1. Introduction.

In this article we study coupled physics electrical conductivity imaging, in which the interactions between the electric and some other fields, such as electromagnetic or acoustic, are utilized, thereby providing useful interior functionals. Coupling the physical fields is advantageous, because it allows for both high spatial and contrast resolutions which are deprived of the traditional electrical impedance tomography. Current density impedance imaging (CDII) (see, e.g., [21]) is one of the coupled physics imaging modalities which has emerged recently in medical diagnostics (see, e.g., [2]). In this article, CDII is understood in the sense that an underlying inverse conductivity problem is formulated as follows.

Let $\Omega \subset R^n, n \geq 2$, be a smooth domain with the connected Lipschitz boundary $\partial\Omega$, the electrical conductivity σ is supposed to be scalar, positive, essentially bounded, and bounded away from zero. Imposing the voltage potential f on $\partial\Omega$ generates in Ω the electric field whose interior voltage potential u satisfies the problem

$$\nabla \cdot (\sigma(x)\nabla u) = 0 \quad \text{in } \Omega, \tag{1.1}$$

$$u = f \quad \text{on } \partial\Omega. \tag{1.2}$$

In turn, the electric field generates in Ω a current density field in accordance with Ohm's law $J = -\sigma\nabla u$. Recall that if $f \in H^{1/2}(\partial\Omega)$, then this problem has a unique weak solution $u \in H^1(\Omega)$. In practice, the boundary data f are at our disposal, and the interior data $|J|$ can be obtained from magnetic resonance measurements (see, e.g., [30]). Given the data $(f, |J|)$, find the pair of functions (u, σ) in Ω.

*Submitted to the journal's Computational Methods in Science and Engineering section January 2, 2019; accepted for publication (in revised form) September 9, 2019; published electronically DATE.
https://doi.org/10.1137/18M1236071
Funding: This work was supported by the NSF under grant DMS-1818882.
†Division of Mathematics and Computer Science, University of South Carolina Upstate, Spartanburg, SC 29303 (atimonov@uscupstate.edu), the Steklov Institute of Mathematics (S. Petersburg branch), S. Petersburg, Russia (altim@pdmi.ras.ru).

Representing $\sigma = |J|/|\nabla u|$ in accordance with Ohm's law, the problem (1.1)–(1.2) can be recast as the weighted 1-Laplacian

$$\nabla \cdot \left(|J|(x) \frac{\nabla u}{|\nabla u|} \right) = 0 \text{ in } \Omega \tag{1.3}$$

subject to (1.2). However, it was shown in [20] that due to the singularity and elliptic degeneracy of the differential operator in the left-hand side of (1.3), it may have no solutions or there are many solutions. Therefore, the weighted least gradient Dirichlet problem

$$argmin \left\{ \int_\Omega |J||\nabla u| dx : u \in W^{1,1}_+(\Omega) \cap C(\overline{\Omega}), u = f \text{ on } \partial\Omega \right\} \tag{1.4}$$

was chosen as a mathematical model of CDII. We denote $W^{1,1}_+(\Omega)$ the space of $L_1(\Omega)$ maps with gradients in $L_1(\Omega)$ for which the set of points where the gradients vanish has at most Lebesgue measure zero. It was proved in [20] that if $f \in C^{1,\nu}(\partial\Omega)$, $|J| \in C^\nu(\Omega)$, $\nu \in (0,1)$, and $|J| > 0$ a.e. in Ω, and the data $(f, |J|)$ are admissible, i.e., there exists a positive conductivity σ that is essentially bounded and bounded away from zero, such that if $u \in H^1(\Omega)$ is a weak solution to the problem (1.1)–(1.2) then $|J| = \sigma|\nabla u|$, then the problem (1.4) is uniquely solvable in $W^{1,1}(\Omega) \cap C(\overline{\Omega})$, and $\sigma = |J|/|\nabla u|$ is Hölder continuous. It was also shown that (1.3) is, formally, the Euler–Lagrange equation of the energy functional in (1.4) and that the solution of the variational problem (1.4) is a weak solution to (1.3). Later, the existence and uniqueness results were established in [12, 19] for the general weighted least gradient problems in $BV(\Omega)$:

$$argmin \left\{ \int_\Omega a(x)|Du| : u \in BV(\Omega), u = f \text{ on } \partial\Omega \right\}, \tag{1.5}$$

where either $a \in C^{1,1}(\Omega)$, $f \in C(\partial\Omega)$ [12] or $a \in C(\Omega)$, $a \geq 0$, and the pair $(f, |J|)$ is admissible [19]. Based on these results, as well as on convexity of the energy functional, two computational algorithms [18, 20] for solving the problem (1.4) were developed and used for reconstructions of the planar conductivity from the data $(f, |J|)$.

Unlike the weighted least gradient problems (1.4), (1.5), in this article for an arbitrary $T > 0$ we introduce the level set representation of the weighted mean curvature flow (MCF) equation

$$u_t = |\nabla u| \nabla \cdot \left(|J|(x) \frac{\nabla u}{|\nabla u|} \right) \text{ in } Q_T = \Omega \times (0, T], \tag{1.6}$$

which is relevant to (1.3). Each level set of u evolves in accordance with the weighted mean curvature

$$H = \nabla \cdot \left(|J|(x) \frac{\nabla u}{|\nabla u|} \right).$$

Introducing such an evolution model is motivated by the following. It is well known that the MCF equation, i.e., (1.6) with $|J| \equiv 1$, received a lot of attention in differential geometry in relation to motion of the level sets of the solution by mean curvature. It has also been of particular interest in many applications of fluid dynamics, combustion, and image processing. In the earlier works of Osher and Sethian [24], Sethian [31], and Alvarez, Lions, and Morel [1] the level set representation of the

MCF equation was utilized for propagating interfaces and image selective smoothing and edge detection. In particular, it was observed in [1] that the mean curvature diffuses u in the direction orthogonal to ∇u, whereas diffusion does not take place in the direction of ∇u. This property is widely used in image processing for improving the spatial resolution of an image. Also, the evolution of $u(x,t)$ can be considered as a smoothed field of a certain initial condition u_0, which is dissipated at a sufficiently large time T. The theoretical justification of the Osher–Sethian approach was given by Evans and Spruck [8, 9, 10] and Chen, Giga, and Goto [6] for the Cauchy problem for the MCF equation. They established the existence and uniqueness results based on the concept of viscosity solutions [7].

In [32] Sternberg and Ziemer investigated the MCF equation subject to the boundary and initial conditions

$$u = f(x) \qquad \text{on } \partial\Omega \times (0,T], \tag{1.7}$$

$$u = u_0(x) \qquad \text{in } \overline{\Omega} \times \{0\} \tag{1.8}$$

under an assumption that the boundary $\partial\Omega$ has positive mean curvature. By analogy, we consider the initial boundary value problem (1.6)–(1.8) as an evolution model of CDII. As in [32], we assume that the weighted mean curvature H is positive, so that the lateral boundary condition (1.7) holds in the classical sense.

However, it was shown in [32] that there exists a continuum of equilibria for the flow described by (1.6)–(1.8) with $|J| \equiv 1$, among which there is only one function of least gradient. This means that uniqueness of viscosity solutions to the problem (1.6)–(1.8) cannot be guaranteed. That is, this problem is ill-posed in the sense of Hadamard. Therefore, we regularize this problem as follows. Following [8], the term $|\nabla u|$ is approximated by the ε-parametric functions

$$g_\varepsilon(|\nabla u|) = (\varepsilon^2 + |\nabla u|^2)^{1/2}, \quad \varepsilon > 0.$$

To treat the degeneracy of the differential operator, we add the viscosity term $\alpha\Delta u$, $0 < \alpha < 1$, to the weighted mean curvature following [23]. As a result, for an arbitrary $T > 0$ we obtain the regularized weighted MCF problem

$$g_\varepsilon^{-1}(|\nabla u^{(\alpha\varepsilon)}|)u_t^{(\alpha\varepsilon)} = \nabla \cdot \left[\sigma(x, |\nabla u^{(\alpha\varepsilon)}|)\nabla u^{(\alpha\varepsilon)}\right] \qquad \text{in } Q_T, \tag{1.9}$$

$$u^{(\alpha\varepsilon)}(t,x) = f(x) \qquad \text{on } \partial\Omega \times (0,T], \tag{1.10}$$

$$u^{(\alpha\varepsilon)}(x,0) = u_0(x) \qquad \text{in } \overline{\Omega} \times \{0\}, \tag{1.11}$$

where

$$\sigma(x,p) = \frac{|J|(x)}{g_\varepsilon(p)} + \alpha, \quad p = |\nabla u^{(\alpha\varepsilon)}|.$$

Also we assume that the compatibility condition is satisfied, i.e., the function $f(x)$ on the lateral surface $\partial\Omega \times (0,T]$ is the trace of $u_0(x)$ on the boundary $\partial\Omega$. Once the solution $u^{(\alpha\varepsilon)}$ of the problem (1.9)–(1.11) is found, we define the regularized solution of the coupled physics inverse conductivity problem as the pair $(u^{(\alpha\varepsilon)}, \sigma^{(\alpha\varepsilon)})$, where

$$\sigma^{(\alpha\varepsilon)} = |J|/|\nabla u^{(\alpha\varepsilon)}|.$$

By analogy with [10], we think of

$$H_{\alpha\varepsilon} = \nabla \cdot \left(|J| \frac{\nabla u^{(\alpha\varepsilon)}}{\sqrt{\varepsilon^2 + |\nabla u^{(\alpha\varepsilon)}|^2}} \right)$$

as being the approximate weighted mean curvature for the level sets of $u^{(\alpha\varepsilon)}$.

In this article, the subject of our consideration is the problem (1.9)–(1.11). The reason is twofold. First, due to the ill-posedness of the problem (1.6)–(1.8), computations cannot be performed without its regularization. Second, the results of the numerical study can be used to formulate conjectures for further analysis of regularity conditions for the problem (1.6)–(1.8). The numerical study is aimed at the central question of whether the sequence of regularized solutions $u^{(\alpha\varepsilon)}$ will approach the function u^* of the weighted least gradient as the parameters ε and α approach zero at a sufficiently large time T.

To the best of the author's knowledge, there are no publications available in the mathematics literature on the methods and algorithms for the numerical solution of the problem (1.6)–(1.8). In the case $|J| \equiv 1$, along with the algorithms for propagating interfaces developed in [24] and [31], there are several algorithms developed for image processing. In [1] the semi-implicit method of discretization in t was directly applied to the MCF equation subject to the homogeneous Neumann boundary condition, and the degenerate diffusion operator $|\nabla u|\nabla \cdot (\nabla u/|\nabla u|)$ was approximated on a grid by the finite differences. Based on the direct application of the finite element method to the MCF equation, an algorithm was developed in [34], though uniqueness was not theoretically guaranteed. This drawback was eliminated in subsequent works [15] and [14] where a combination of schemes from [1] and [34] was presented. In [22] an explicit convergent finite-difference scheme was developed but it suffers from low accuracy.

Unlike the approaches indicated above, our approach is not based on the theory of viscosity solutions, and we do not apply the finite element method to the evolution equation, as well as we do not approximate directly the degenerate diffusion operator by finite differences. Instead, we first eliminate both the singularity and degeneracy of the differential operator in (1.6), thereby approximating the ill-posed problem (1.6)–(1.8) by a family of quasi-linear parabolic problems (1.9)–(1.11) whose unique solvability in an appropriate Hőlder space follows from Ladyzhenskaya's theory [16]. In other words, we approximate the originally ill-posed problem by a family of well-posed problems. Then, by applying Rothe's method to the regularized problem (1.9)–(1.11) with the fixed parameters ε and α, we transform it to a family of second-order linear elliptic problems, the finite-difference schemes of which are well studied and available in the mathematics literature (see, e.g., [5, 13, 26, 27, 28]). Note that applicability of the Rothe's method to the regularized problem (1.9)–(1.11), as well as its convergence, follows directly from the results by Ladyzhenskaya [17] and Ventzel [33].

As mentioned above, in our further analytical investigation the $\alpha\varepsilon$-regularization is going to be used to obtain existence and uniqueness for the weighted MCF problem (1.6)–(1.8) by passing the sequence $u^{(\alpha\varepsilon)}$ to the double limit as $\alpha, \varepsilon \to 0$. This implies that in the presented numerical study of the regularized problem (1.9)–(1.11) the positive parameters α and ε are fixed and they can be taken arbitrarily close to zero. The question of a special choice of these parameters (e.g., like in Tikhonov's regularization), being interesting by itself, is beyond the scope of this paper.

The paper is formatted as follows. In the next section, we discuss briefly the issues of existence and uniqueness of the weak and classical solutions of the regularized weighted MCF problem. In section 3 we apply Rothe's method to this problem. In section 4 we present the finite-difference approximation of an elliptic problem resulting from applying Rothe's method and outline the resularized successive approximations. In section 5 we demonstrate and discuss some results of the numerical study. Finally, we conclude our investigation in section 6 and formulate two conjectures for further analysis.

2. On the well posedness of the regularized weighted MCF problem. Let $\Omega \subset R^n$ be a bounded domain and $\partial(\Omega)$ be a sufficiently smooth boundary with positive weighted mean curvature. Since in general the function $|J|(x)$ may be discontinuous, a classical solution to the regularized weighted MCF problem (1.9)–(1.11) may not necessarily exist. Therefore, we first consider a weak solution to this problem. In accordance with the standard definition, it is a function $u^{(\alpha\varepsilon)} \in C([0,T];H^1(\Omega))$, such that for all test functions $w \in H^{1,2}(Q_T)$ vanishing on $\partial\Omega \times (0,T)$ and on $\Omega \times \{T\}$ it satisfies the identity

$$\int_{Q_T} \left[-g_\varepsilon^{-1} u^{(\alpha\varepsilon)} w_t + \sigma \nabla u^{(\alpha\varepsilon)} \cdot \nabla w \right] dxdt - \int_\Omega g_\varepsilon^{-1} u_0 w(x,0) dx = 0$$

and the condition (1.10). Here,

$$H^{1,2}(Q_T) = \left\{ w(t,x) : \frac{\partial w}{\partial t} \in L_2((0,T);L_2(\Omega)), w \in L_2((0,T);W_2^2(\Omega)) \right\}.$$

The existence and uniqueness results for the linear and quasilinear parabolic problems were established by Ladyzhenskaya (see, e.g., [16]). Here we indicate these results in relation to the problem (1.9)–(1.11).

PROPOSITION 2.1. *Suppose* $f \in H^{1/2}(\partial\Omega)$, $|J| \in L_\infty(\Omega)$, $|J| > 0$, *and* $u_0 \in L_2(\Omega)$. *Then for the fixed* $0 < \alpha < 1$, $\varepsilon > 0$, *there exists a unique weak solution* $u^{(\alpha\varepsilon)} \in C([0,T];H^1(\Omega))$ *to the problem* (1.9)–(1.11).

Taking into account the compatibility condition on $\partial\Omega$, in accordance with the maximum principle, we obtain

$$\|u^{(\alpha\varepsilon)}\|_{L_\infty(Q_T)} \le \|u_0\|_{L_\infty(\Omega)}.$$

If the Hölder regularity conditions are satisfied, i.e.,

1. $\partial\Omega \in C^{2,\nu}$,
2. $f \in C^{2,\nu}(\partial\Omega)$, $u_0 \in C^{2,\nu}(\Omega)$,
3. $|J| \in C^{1,\nu}(\Omega)$,

then, representing (1.9) in the nondivergent form

$$\begin{aligned} u_t^{(\alpha\varepsilon)} &= g_\varepsilon(|\nabla u^{(\alpha\varepsilon)}|) \left\{ \sum_{i,j=1}^n \sigma(x;|\nabla u^{(\alpha\varepsilon)}|)\delta_{ij} u_{x_i x_j}^{(\alpha\varepsilon)} + \sum_{i=1}^n \sigma_{x_i} u_{x_i}^{(\alpha\varepsilon)} \right\} \\ &= \sum_{i,j=1}^n |J|(x) \left[(1+\alpha \frac{g_\varepsilon(|\nabla u^{(\alpha\varepsilon)}|)}{|J|(x)})\delta_{ij} - \frac{u_{x_i}^{(\alpha\varepsilon)} u_{x_j}^{(\alpha\varepsilon)}}{\varepsilon^2 + |\nabla u^{(\alpha\varepsilon)}|^2} \right] u_{x_i x_j}^{(\alpha\varepsilon)} \\ &\quad + \sum_{i=1}^n |J|_{x_i} u_{x_i}^{(\alpha\varepsilon)}, \end{aligned} \tag{2.1}$$

where δ_{ij} is the Kronecker symbol, we obtain from [16, Chapter VI, Theorem 4.2] that the regularized weighted MCF problem has a unique classical solution $u^{(\alpha\varepsilon)} \in C^{2+\nu,1+\nu/2}(Q_T)$, and the following bound takes place:

$$\|u\|_{C^{2+\nu,1+\nu/2}(Q_T)} \le C\|u_0\|_{C^{2,\nu}(\Omega)},$$

where $C = const > 0$ that does not depend on t. Recall that a classical solution of the problem is also a weak solution.

From both the analytical and computational points of view, it is convenient to represent the solution of the problem (1.9)–(1.11) as

$$u^{(\alpha\varepsilon)}(x,t) = v(x,t) + u_h(x), \tag{2.2}$$

where the function u_h solves an auxiliary problem

$$\Delta u_h = 0 \ \text{ in } \Omega, \tag{2.3}$$

$$u_h = f \ \text{ on } \partial\Omega. \tag{2.4}$$

The harmonic function u_h represents the "stationary" voltage potential induced by the given boundary voltage f in the domain Ω filled with the homogeneous conductive medium with $\sigma = 1$, whereas the voltage potential $v(x,t)$ evolves being modulated by $|J|$. By setting $u_0 = u_h$, the problem (1.9)–(1.11) is transformed to the initial boundary value problem with the homogeneous conditions

$$\begin{aligned}\frac{\partial v}{\partial t} = g_\varepsilon(|\nabla(u_h+v)|)\{\nabla\cdot(\sigma(x,|\nabla(u_h+v)|)\nabla v)\\ + \nabla\cdot(\sigma(x,|\nabla(u_h+v)|)\nabla u_h)\} \ \text{ in } Q_T,\end{aligned} \tag{2.5}$$

$$v(x,t) = 0 \ \text{ on } \partial\Omega\times(0,T), \tag{2.6}$$

$$v(x,0) = 0 \ \text{ in } \overline{\Omega}\times\{0\}. \tag{2.7}$$

As was shown in [17], vanishing $v(x,t)$ on the lateral surface of the cylinder Q_T is required for establishing convergence of Rothe's method.

3. Applying Rothe's method. The choice of Rothe's method [25] for the numerical solution of the problem (2.5)–(2.7) is motivated by the fact that Ladyzhenskaya [17] and Ventzel [33] used it for the first time for establishing the existence and uniqueness results for quasi-linear parabolic equations with the Dirichlet boundary condition. Their proofs are constructive in the sense that they rely on the existence of a limit of the sequence of Rothe's functions. In other words, the convergence of this sequence naturally follows from the Ladyzhenskaya–Ventzel technique of proving existence and uniqueness of the initial boundary value problem for quasi-linear parabolic equations. We use this observation in relation to the problem (2.5)–(2.7).

According to Rothe's method, we intersect cylinder Q_T by hyperplanes $t_k = k\tau$, $\tau = T/K$ $(k = 0,1,\ldots,K)$. Let Ω_k be its kth cross section. For $t = t_k$ we define the function $v_\tau(x,t_k)$ that satisfies the linear elliptic equation

$$\begin{aligned}(v_\tau)_{\overline{t}}(x,t_k) = g_\varepsilon(|\nabla(u_h+v^{(k-1)})|)\{\nabla\cdot(\sigma(x,|\nabla(u_h+v^{(k-1)})|)\nabla v^{(k)})\\ + \nabla\cdot(\sigma(x,|\nabla(u_h+v^{(k-1)})|))\nabla u_h\} \ \text{ in } \Omega_k,\end{aligned} \tag{3.1}$$

subject to the Dirichlet condition

$$v_\tau^{(k)} = 0 \ \text{ on } \partial\Omega_k, \tag{3.2}$$

where $v^{(k)}(x) = v_\tau(x,t_k)$, and the temporal derivative in the left-hand side of (2.5) is approximated by the backward difference formula

$$(v_\tau)_{\overline{t}}(x,t_k) = \frac{v^{(k)}(x) - v^{(k-1)}(x)}{\tau}.$$

Thus, for any fixed integer K we obtain the finite sequence $\{v^{(k)}(x)\}$ of solutions to the elliptic problems (3.1)–(3.2). Let $\{v_\tau(x,t)\}$ be a sequence of functions $v_\tau(x,t), (x,t) \in Q_T$, such that $v_\tau(x,0) = 0$. As an example, we indicate Rothe's function, i.e., the linear interpolant in t,

$$v_\tau(x,t) = v^{(k-1)}(x) + \frac{t - t_{k-1}}{\tau}(v^{(k)}(x) - v^{(k-1)}(x)) \ \text{ for } t_{k-1} \le t \le t_k. \tag{3.3}$$

In [17] and [33] the global existence and uniqueness of both the classical and weak solutions of quasi-linear parabolic equations were established by passage $v_\tau(x,t)$ to the limit as $\tau \to 0$. Utilizing the Ladyzhenskaya–Ventzel technique, convergence of Rothe's method can also be established for our case.

PROPOSITION 3.1. *Suppose Ω is a bounded domain with the $C^{2,\nu}$-boundary, and $|J| \in C^{1,\nu}(\Omega)$. Then for an arbitrary $T > 0$ and fixed parameters $0 < \varepsilon < 1,\ 0 < \alpha < 1$, the sequence of Rothe's functions $\{v_\tau(x,t)\}$ converges uniformly in the t-variable to the unique weak solution $v(x,t)$ of the problem (2.5)–(2.7) as $\tau \to 0$.*

The proof is analogous to that given in [17] and it is based on the Schauder theory [11, 29] for an elliptic Dirichlet problem (3.1)–(3.2) and on a priori estimates for the problem (2.5)–(2.7):

$$|v_\tau| \le c_1,$$

$$\left|\frac{\partial v_\tau}{\partial x_i}\right| \le c_2,$$

$$\tau \sum_{k=1}^{K} \int_\Omega \left\{ v^2_{\tau\overline{t}}(x,t_k) + \sum_{i,j=1}^{n} (\partial^2_{x_i x_j} v_\tau(x,t_k))^2 + \tau \sum_{i=1}^{n} (\partial_{x_i} v_{\tau\overline{t}}(x,t_k))^2 \right\} dx \le c_3,$$

where $c_1, c_2, c_3 > 0$ are constants which do not depend on τ, as well as on the uniqueness result for (2.5)–(2.7).

Also, it follows directly from [17] and [33] that if $|J|(x) \in C^{4,\nu}(\Omega)$, then the limit function $v(x,t)$ is the classical solution of the problem (2.5)–(2.7).

4. On the numerical solution to the elliptic problem (3.1)–(3.2). Rothe's method reduces the quasi-linear problem (1.9)–(1.11) to a family of linear elliptic problems (3.1)–(3.2) with the homogeneous boundary conditions. For every $t = t_k,\ k \ge 1$, we rewrite (3.1)–(3.2) as

$$-\sum_{i=1}^{n} \frac{\partial}{\partial x_i}\left(\sigma^{(k-1)} \frac{\partial v_\tau^{(k)}}{\partial x_i}\right) + q^{(k-1)}(x) v_\tau^{(k)} = F^{(k-1)}(x) \ \text{ in } \Omega_k, \tag{4.1}$$

$$v_\tau^{(k)} = 0 \ \text{ on } \partial\Omega_k, \tag{4.2}$$

where

$$g_\varepsilon^{(k)} = g_\varepsilon(|\nabla(u_h + v^{(k)})|),$$

$$\sigma^{(k)} = \frac{|J|(x)}{g_\varepsilon^{(k)}} + \alpha,$$

$$q^{(k)} = \frac{1}{\tau g_\varepsilon^{(k)}},$$

$$F^{(k)} = \nabla \cdot (\sigma^{(k)} \nabla u_h) + q^{(k)} v_\tau^{(k)}.$$

Under the conditions indicated in the previous section, a priori estimate $|v_\tau(x,t_k)| \le C,\ C>0$, takes place for all $t_k \le T$. According to Schauder's theory [11, 29], it ensures the unique solvability of the problem (4.1)–(4.2).

In the mathematics literature there are available several efficient finite-difference schemes (see, e.g., [5, 13, 26, 27, 28]). Without loss of generality, consider the problem (4.1)–(4.2) in two dimensions and approximate it by its difference analogue following [27]. Let $\overline{\Omega}_k$ be a unit square,

$$\overline{\Omega}_k = \{(x_1,x_2) : 0 \le x_i \le 1,\ (i=1,2)\},$$

on which we define the uniform grids

$$\overline{g} = \{(x_1,x_2) : x_{1l} = lh,\ x_{2m} = mh,\ hN = 1,\ (l,m = 0,1,\dots,N)\},$$
$$g = \{(x_1,x_2) : x_{1l} = lh,\ x_{2m} = mh,\ hN = 1,\ (l,m = 1,2,\dots,N-1)\},$$

so that $\gamma = \overline{g} \setminus g$ is the discrete boundary. On $\overline{g}$ we introduce the grid function $y = y_{lm}$ and on g we approximate the differential operator in the left-hand side of (4.1) as follows:

$$\hat{L}y = (s_1 y_{\overline{x}_1})_{x_1} + (s_2 y_{\overline{x}_2})_{x_2}, \tag{4.3}$$

where

$$(s_1 y_{\overline{x}_1})_{x_1} = \frac{1}{h^2}[(s_1)_{l+1m}(y_{l+1m} - y_{lm}) - (s_1)_{lm}(y_{lm} - y_{l-1m})],$$
$$(s_2 y_{\overline{x}_2})_{x_2} = \frac{1}{h^2}[(s_2)_{lm+1}(y_{lm+1} - y_{lm}) - (s_2)_{lm}(y_{lm} - y_{lm-1})],$$
$$(s_1)_{lm} = \frac{1}{2}[\sigma(x_{1l-1},x_{2m}) + \sigma(x_{1l},x_{2m})],$$
$$(s_2)_{lm} = \frac{1}{2}[\sigma(x_{1l},x_{2m-1}) + \sigma(x_{1l},x_{2m})].$$

Denoting $\hat{q} = q(x_{1l},x_{2m})$, $\hat{F} = F(x_{1l},x_{2m})$, we arrive at the following difference scheme

$$-Ly + \hat{q}y = \hat{F}, \qquad x \in g, \tag{4.4}$$
$$y = 0, \qquad x \in \gamma. \tag{4.5}$$

It follows from [27] that this difference scheme approximates the problem (4.1)–(4.2) to second order. If $v(x,t)$ is the classical solution to this problem, then it follows from [27] that the solution of the difference problem (4.4)–(4.5) converges in the discrete L_2 and W_2^1 norms, and the error bounds are given by

$$\|y - \hat{v}\|_{L_2} \le \mu_1 h^2, \quad \|u - \hat{v}\|_{W_2^1} \le \mu_2 h^{3/2} \text{ if } |J|(x) \text{ is smooth},$$
$$\|u - \hat{v}\|_{W_2^1} \le \mu_3 h^{1/2} \text{ if } |J|(x) \text{ is discontinuous},$$

where $\hat{v} = v(x_{1l},x_{2m})$ and the constants $\mu_1,\mu_2,\mu_3 > 0$ do not depend on h. Similar error bounds take place in the case of a weak solution (see [13]).

Let H be a set of all discrete functions y on $\overline{g}$ which vanish on γ. If we introduce in H the norm and scalar product as

$$\|z\| = (z,z)^{1/2},\ (z,w) = h^2 \sum_{l,m=1}^{N} z_l w_m,$$

then the set H becomes a Hilbert space, and one can describe the difference scheme (4.4)–(4.5) as the operator equation

$$Dy = \hat{F}, \quad y, \hat{F} \in H, \tag{4.6}$$

where

$$Dy = -[(s_1 y_{\overline{x}_1})_{x_1} + (s_2 y_{\overline{x}_2})_{x_2}] + \hat{q}y.$$

Using the difference analogue of the Greens' formula, one can easily show that the operator $D : H \to H$ is positive definite and self-adjoint. Hence, the corresponding matrix D is symmetric and positive definite, so that its spectrum consists of positive real eigenvalues and it is bounded for any fixed N. In this case there exists a bounded inverse D^{-1} of D on H, i.e., the operator equation (4.6) has a unique solution. The corresponding matrix D is a special band symmetric matrix that consists of five diagonals. Nonzero entries of D are located on the main diagonal, on two super- and sub-diagonals adjacent to the main one, and on two remote diagonals located symmetrically with respect to the main one, so that its bandwidth is equal to the distance between the main diagonal and any of the remote diagonals.

It is observed in the numerical experiments that for the sufficiently small parameters α and ε and step size h and for a sufficiently large local variation of $\sigma^{(k)}$ (a high contrast) a small change in entries of D and in the right-hand side $\hat{F}$ may cause a significant change in the solution of (4.6). Under this condition, the Krylov subspace methods, e.g., conjugate gradient method, either do not ensure the convergence or possess extremely low rates of convergence. There is available in the mathematics literature a variety of preconditioning techniques (see, e.g., surveys in [3, 4]) which ensure the efficient computations at a reasonable cost and, therefore, they may be used for the numerical solution of (4.6). In our numerical experiments we use an implicit version of the preconditioned conjugate gradient method (see, e.g., [28]), in which the error of each iteration is minimized in the energy norm, and the correction vector from the Krylov subspace is determined.

5. Numerical study. In this section we study some properties of the numerical solutions to the regularized weighted MCF problem. All computations were performed with double precision on the Dell Precision workstation T5400 running under IDL.

5.1. Data simulations. In computer simulations we consider a planar domain $\Omega = (0,1) \times (0,1)$. To simulate the conductivity distribution in Ω, we use two model functions. The first C^∞-smooth model function is given by

$$\begin{aligned}\sigma(x_1, x_2) &= 1.1 + 0.3\Big\{0.3(1-3z)^2 \cdot \exp[2z^2 + (3w-2)^2] - \left(\frac{3}{5}z - 27z^3 - (3(w-1))^5\right) \\ &\qquad \cdot \exp[9z^2 + 9(w-1)^2] - \exp[(3z+1)^2 + 9(w-1)^2]\Big\},\end{aligned}$$

where $z = 2x_1 - 1,\ w = 2x_2$. The second model function is constructed from a real abdominal computed tomography (CT) image of a human, which we embed into Ω. The actual Hounsfield units are rescaled of the realistic range [1, 1.8] S/m of the electrical conductivity typical of the biological tissues. Due to the pixel structure of a CT image, the second model function is discontinuous. For both model functions, the conductivity bounds are chosen as $\underline{\sigma} = 0.9$ S/m and $\overline{\sigma} = 2$ S/m. In a planar domain a two-to-one map f ensures the positivity of $|J|$ almost everywhere in Ω [20].

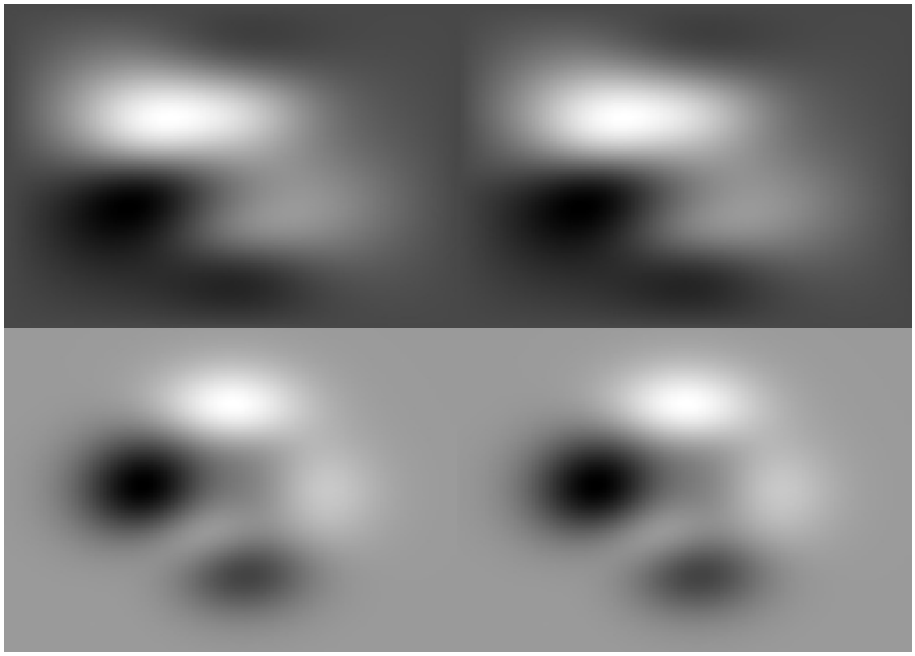

FIG. 1. *A C^∞-smooth model. Figures go from top to bottom and from left to right. In the first column: u^* and σ^* for the two-to-one boundary map. In the second u^* and σ^* for the many-to-one boundary map, $A = 0.1, k = 9$.*

Recall that a map on a connected boundary is said to be two-to-one if the set of local maxima is either one point or one connected arc. To simulate the boundary voltage potential f, we use two continuous functions defined on sides on the unit square. One of these functions is two-to-one,

$$f_1(x_1, x_2) = x_2,$$

whereas another one is many-to-one,

$$f_2(x_1, x_2) = f_1(x_1, x_2) + A\sin(k\pi x_2),$$

where $0 < A < 1$ is a real number and $k \geq 2$ is an integer.

Given the pair (σ, f), the standard Galerkin finite element method is used to solve numerically the forward problem (1.1)–(1.2). Let u_s be its solution. Then the simulated interior data are computed as $|J| = \sigma|\nabla u_s|$ in order to ensure the admissibility. To provide an appropriate accuracy, the basis elements and mesh density are carefully chosen. In the numerical experiments with several test problems we have found that using the first-order element basis with the number of elements of order of tens of thousands allows for a small relative error of order 10^{-5}. The simulated data $(f, |J|)$ are first used to find the weighted least gradient function u^* and the corresponding conductivity σ^*. The Picard-like algorithm from [20] is used to minimize the energy functional in (1.4) for f_1. In the case of the many-to-one function f_2 the alternating split Bregman algorithm developed in [18] is utilized, because it provides higher accuracy. The pairs of functions (u^*, σ^*) for the smooth conductivity model are shown in Figure 1. In Figure 2 the corresponding pairs are shown for the discontinuous conductivity model.

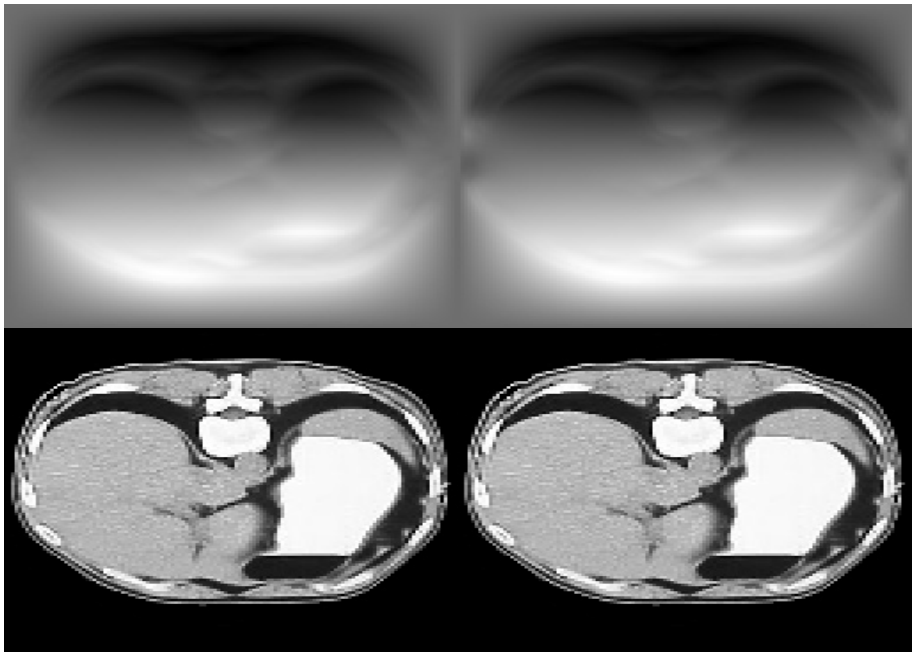

FIG. 2. *A realistic discontinuous model. Figures go from top to bottom and from left to right. In the first column: u^* and σ^* for the two-to-one boundary map. In the second column: u^* and σ^* for the many-to-one boundary map, $A = 0.1, k = 9$.*

5.2. Large time behavior of the regularized solutions. As an alternative to the weighted least gradient Dirichlet problem for conductivity imaging (1.4), we propose using the weighted MCF problem (1.6)–(1.8). However, it was shown in [32] that even for $|J| \equiv 1$ there is a continuum of equilibria for the flow described by (1.6)–(1.8). Because this is important, we reproduce here an example of nonuniqueness from [32].

Let $\mu, |\mu| \leq 1$ be a numerical parameter. Then the μ-parametric family of functions

$$u_\mu(x_1, x_2) = \begin{cases} 2x_1^2 - 1 & \text{if } |x_1| \geq \sqrt{\frac{1+\mu}{2}},\ |x_2| \leq \sqrt{\frac{1-\mu}{2}}, \\ \mu & \text{if } |x_1| \leq \sqrt{\frac{1+\mu}{2}},\ |x_2| \leq \sqrt{\frac{1-\mu}{2}}, \\ 1 - 2x_2^2 & \text{if } |x_1| \geq \sqrt{\frac{1+\mu}{2}},\ |x_2| \geq \sqrt{\frac{1-\mu}{2}}, \end{cases} \tag{5.1}$$

are equilibria for the problem (1.6)–(1.8), i.e., they are viscosity solutions to (1.3) with $|J| \equiv 1$ subject to (1.2). But there is only one function u_μ for $\mu = 0$ that is a solution to the problem (1.4). This means that the flow governed by (1.6)–(1.8) does not necessarily approach a function of the weighted least gradient. Moreover, if we assume that $u_0 = u_\mu$ with $\mu \neq 0$ in (1.6)–(1.8), then

$$\lim_{t\to\infty} \lim_{\varepsilon\to 0} \lim_{\alpha\to 0} u^{(\alpha\varepsilon)} \neq \lim_{\varepsilon\to 0} \lim_{\alpha\to 0} \lim_{t\to\infty} u^{(\alpha\varepsilon)}. \tag{5.2}$$

Clearly, this fact is one of challenges for further analysis of the weighted MCF problem.

In this section we demonstrate in the numerical experiments that for sufficiently small parameters α and ε the level sets of the regularized solutions $u^{(\alpha\varepsilon)}$ are condensed

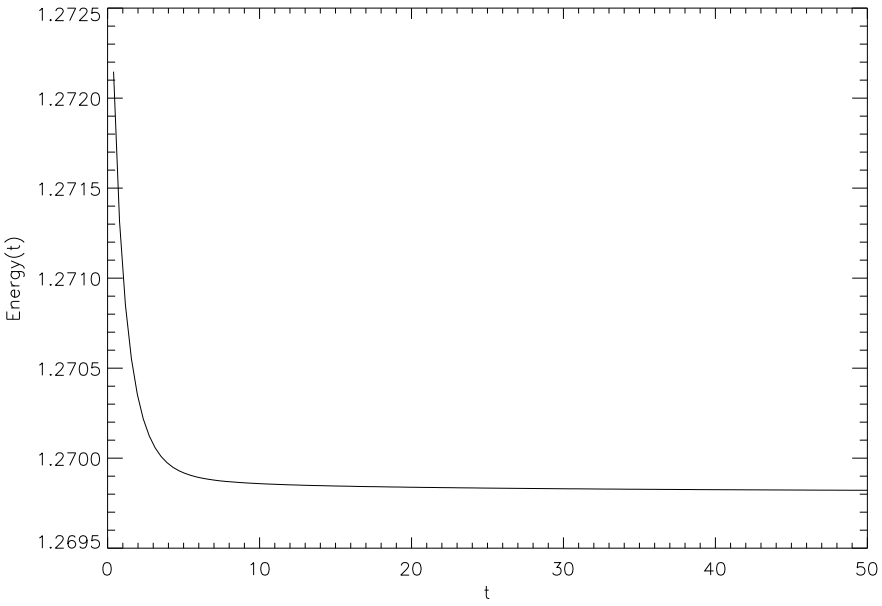

FIG. 3. *The time behavior of the energy functional for* $u_0 = u_h$.

in close proximity of the unique minimizer u^* of the weighted least gradient functional (1.4), i.e., for sufficiently small α and ε at a sufficiently large T we obtain

$$u^{(\alpha\varepsilon)}(x,t) \approx u^*(x), \quad \sigma^{\alpha\varepsilon}(x,t) \approx \sigma^*(x).$$

It was proved in [9] and [32] that the functional

$$\int_\Omega |\nabla u(x,t)|dx$$

is nonincreasing. In Figure 3 we observe even stronger behavior of the energy functional

$$\int_\Omega |J|(x)|\nabla u^{\alpha\varepsilon}(x,t)|dx,$$

which is decreasing. Following [10], one can also show that the functional

$$\int_\Omega |H_{\alpha\varepsilon}(x,t)|dx$$

is nonincreasing in t for any $\alpha, \varepsilon \in (0,1]$ and it is bounded in L_1, i.e.,

$$\sup_{\alpha,\varepsilon\in(0,1]} \sup_{t\geq 0} \int_\Omega |H_{\alpha\varepsilon}(x,t)|dx < \infty.$$

The monotonicity property is important for further analysis of the relation between the limit of $u^{\alpha\varepsilon}$ and a function of the weighted least gradient. Moreover, the relation (5.2) does not take place anymore because of the admissibility condition.

At a consciously large $T = 100$ the α-dependence of the regularized solutions is shown for the discontinuous generating conductivity, many-to-one boundary map f_2 and $\varepsilon = 10^{-5}$ is shown in Figure 4. The ε-dependence for the fixed $\alpha = 10^{-5}$ is

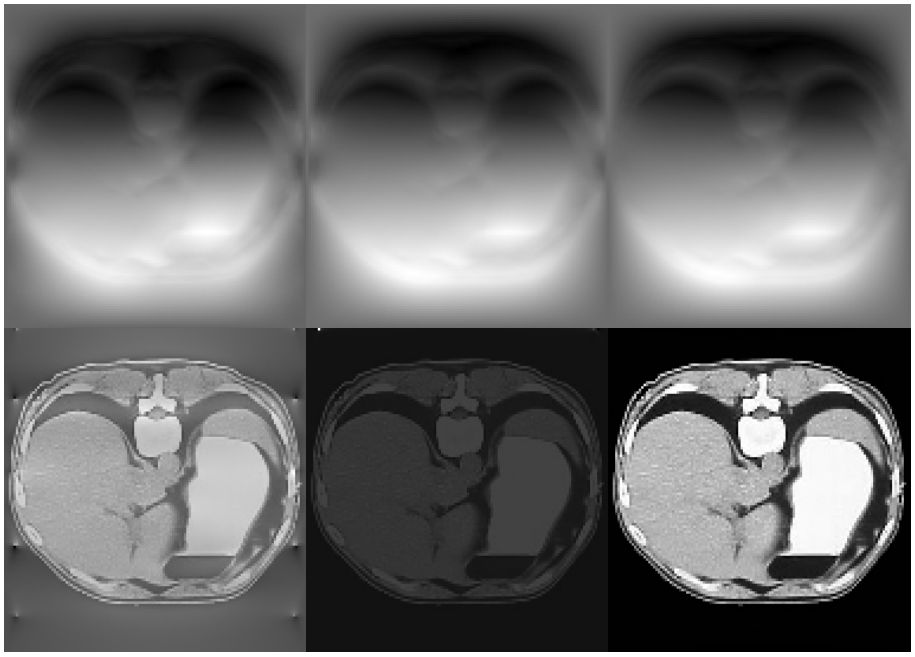

FIG. 4. *Figures go from left to right and from top to bottom. In the first row: the reconstructed voltage potentials* $u^{(\alpha\varepsilon)}$ *for* $\alpha = 10^{-1},\ 10^{-3},\ 10^{-5}$. *In the second row: the corresponding reconstructed conductivities* $\sigma^{(\alpha\varepsilon)}$.

similar. Based on these results, the parameters α and ε have been set to 10^{-5} in the next numerical experiments.

In Figure 5 we show the T-dependence of the relative error

$$E = \frac{\|u^{\alpha\varepsilon} - u^*\|_2}{\|u^*\|_2}$$

for all the model conductivities and boundary maps. We observe that in the case of the unperturbed interior data $|J|$ the relative error attains the level of $1.17 \cdot 10^{-3}$ at $T = 50$ for both the smooth and discontinuous model conductivities and weakly fluctuates around this level with a further increase in T because of the roundoff and truncation errors. In the case of many-to-one boundary map the T-dependence of the relative error is qualitatively the same. However, it attains the levels of $1.84 \cdot 10^{-3}$ and $3.78 \cdot 10^{-3}$ for the smooth and discontinuous conductivities.

Recall that the difference scheme indicated in sections 3 and 4 is homogeneous and implicit. The convergence and accuracy of difference schemes of such types for the quasi-linear parabolic equations were studied in [26]. In particular, it follows from [26] that the step sizes τ and h can be independently chosen. In the following numerical experiments we demonstrate how the temporal step size τ, which is characterized by the Courant number

$$C = \max\left(\sigma(\nabla|u^{(\alpha\varepsilon)}|)\frac{\tau}{h^2}\right),$$

influences the accuracy of $u^{(\alpha\varepsilon)}$ and $\sigma^{(\alpha\varepsilon)} = |J|/|\nabla u^{(\alpha\varepsilon)}|$. For brevity, we show only the numerical results with the two-to-one boundary map for $N = 128$ ($h = 7.81 \cdot 10^{-3}$), though the similar results take place for the many-to-one map. Given the maximum

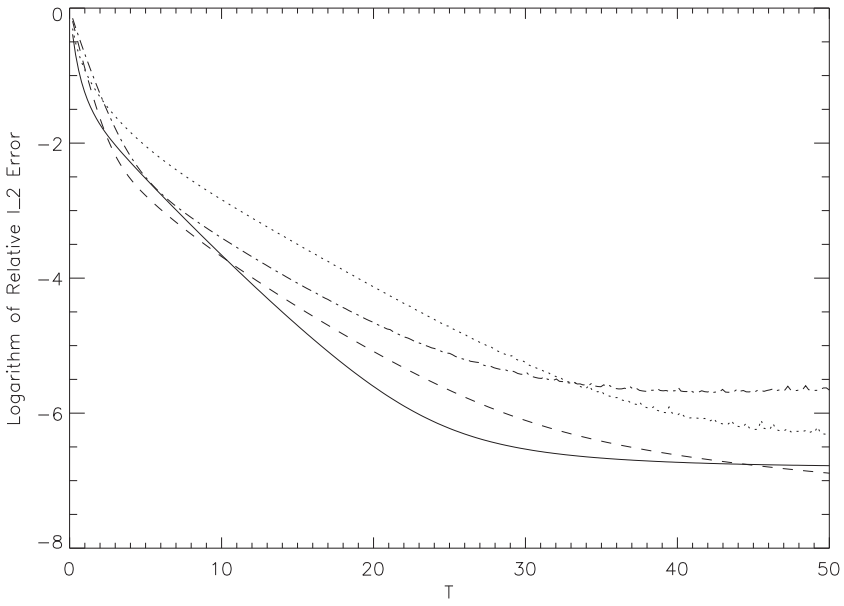

FIG. 5. *Relative error as a function of T: the solid line—for the smooth model conductivity and two-to-one boundary map; the dotted line—for the smooth model conductivity and many-to-one boundary map; the dashed line—for the discontinuous model conductivity and one-to-one boundary map; and the dash dot line—for the discontinuous model conductivity and many-to-one boundary map.*

values of $\sigma^{(\alpha\varepsilon)}$ used in computer simulations, the temporal step sizes were set to 1.56, 0.39, and 0.195, so that the corresponding Courant numbers were 63935, 15983, and 7993. In Figures 6 and 7 the series of regularized solutions $u^{(\alpha\varepsilon)}$ and reconstructed $\sigma^{(\alpha\varepsilon)}$ are shown. We observe that in computations with the finite precision a further increase in T, as well as a decrease in C or τ, does not lead to a significant improvement in accuracy.

5.3. Robustness. To simulate the perturbed interior data $|\tilde{J}|$, we use the simple stochastic model of the additive normally distributed noise

$$|\tilde{J}| = |J| + \delta \cdot \frac{|||J|||_2}{\|R\|_2} R, \tag{5.3}$$

where δ is the prescribed level of error and $R = R(0,1)$ is the normally distributed pseudorandom matrix with the zero mean and standard deviation 1. The original and perturbed interior data with a noise level of 5% for both smooth and discontinuous model conductivities are shown in Figure 8.

Due to the stochastic nature of $|J|$, the pseudorandom matrix R has been generated twenty times and a sample of reconstructed conductivities has been formed for each noise level δ. In Figure 9 the means for every sample are shown for $T = 50$, $K = 256$. As in [1], we observe that the regularized weighted mean curvature term represents an effect that diffuses the voltage potential $u^{(\alpha\varepsilon)}$ in the directions orthogonal to the gradient $\nabla u^{(\alpha\varepsilon)}$ and does not diffuse in the other directions. This means that as $t \to \infty$ the evolution quickly "forgets" about the initial condition $u_0^{(\alpha\varepsilon)}$ and further

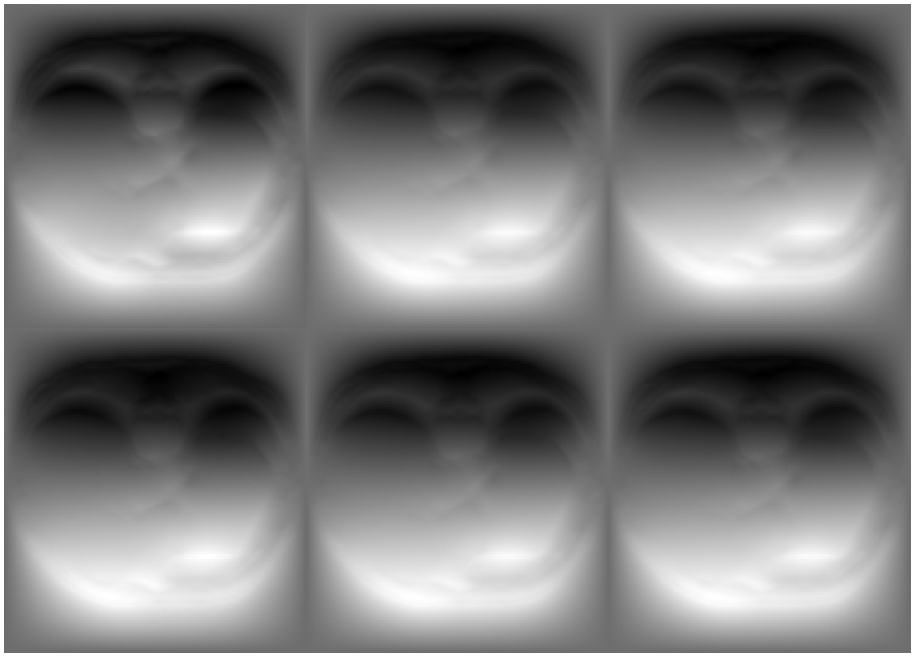

FIG. 6. *Figures go from left to right. In the first row* $u^{(\alpha\varepsilon)}$ *are shown at* $T = 0.1, 1, 50$ *for the fixed* $\tau = 0.195$. *In the second row* $u^{(\alpha\varepsilon)}$ *are shown for* $\tau = 1.56, 0.39, 0.195$ *at the fixed* $T = 50$.

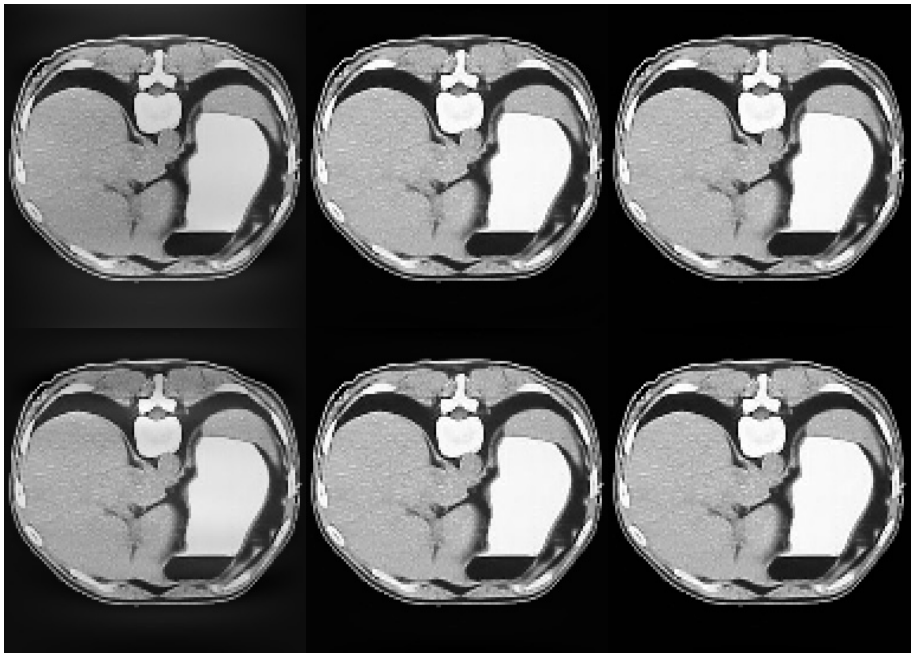

FIG. 7. *Figures go from left to right. In the first row* $\sigma^{(\alpha\varepsilon)}$ *are shown at* $T = 0.1, 1, 50$ *for the fixed* $\tau = 0.195$. *In the second row* $\sigma^{(\alpha\varepsilon)}$ *are shown for* $\tau = 1.56, 0.39, 0.195$ *at the fixed* $T = 50$.

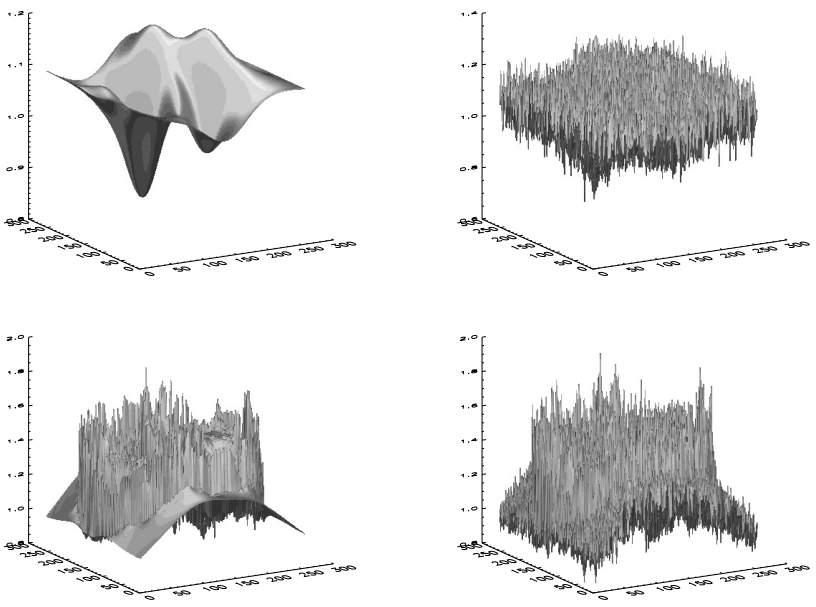

FIG. 8. *Figures go from left to right and from top to bottom. In the first row: the shaded surfaces of* $|J|$ *and* $|\tilde{J}|$ *for the smooth model conductivity. In the second row: the shaded surfaces of* $|J|$ *and* $|\tilde{J}|$ *for the piecewise constant model conductivity.*

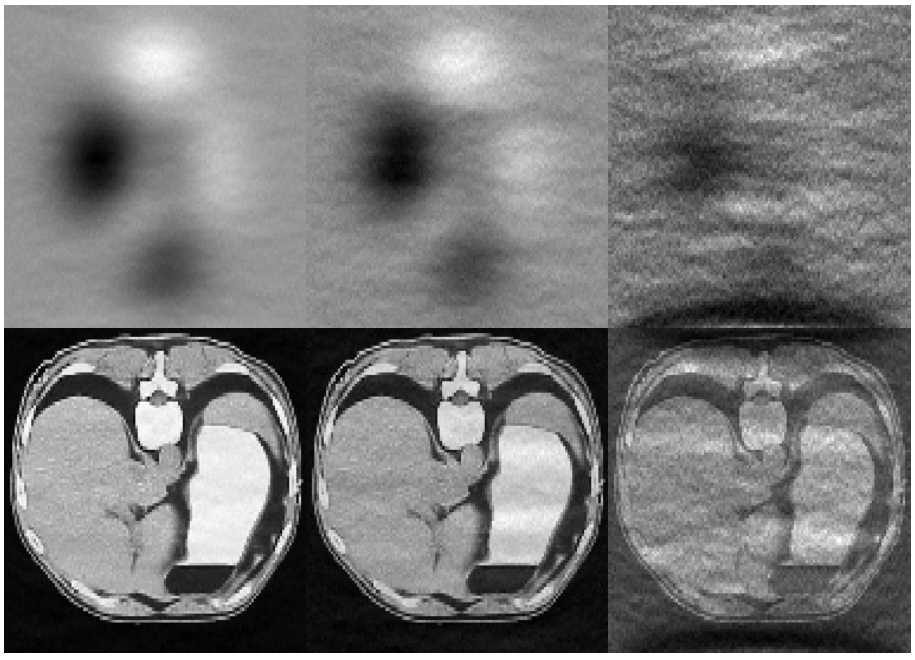

FIG. 9. *Figures go from left to right and from top to bottom. In the first row: means for the smooth model with the* $0.5, 1, 5\%$ *noise level. In the second row: means for the discontinuous model with the* $0.5, 1, 5\%$ *noise level.*

diffuses the voltage potential $u^{(\alpha\varepsilon)}$ everywhere except for some geometrical objects, such as points, lines, etc., where $\nabla u^{(\alpha\varepsilon)}$ is large.

6. Concluding remarks. We have presented a new mathematical model for CDII. The model is based on the regularized weighted MCF equation subject to the boundary and initial conditions. It is an alternative to the weighted least gradient Dirichlet problem currently used in CDII. The reconstruction algorithm based on Rothe's method and second-order finite-difference approximation of the resulting elliptic problems is stable and easy to implement. We have performed the numerical study, in which the feasibility of the alternative model and algorithm was established. In particular, we have demonstrated that at a sufficiently large time the numerical solutions of the regularized weighted MCF problem are in close proximity to the unique solution to the weighted least gradient Dirichlet problem. The numerical evidence of robustness of the proposed algorithm has been obtained. Based on the results of numerical study, we formulate two conjectures for further analysis.

CONJECTURE 1. *Let $\Omega \subset R^n$, $n \geq 2$, be a smooth domain with the connected Lipschitz boundary $\partial\Omega$. Suppose $|J| > 0$ on $\overline{\Omega}$, the data $(f, |J|) \in C^{2,\nu}(\partial\Omega) \times C^{\nu}(\Omega)$ are admissible in the sense of* [20], *and the boundary $\partial\Omega$ has everywhere a positive weighted mean curvature. Then for every fixed $\varepsilon \in (0, 1]$ there exists a function $w^{\varepsilon} \in C^2(\Omega)$ and Lipschitz on $\partial\Omega$, such that* (1) $\lim_{\alpha\to 0} \lim_{t\to\infty} u^{(\alpha,\varepsilon)} = w^{\varepsilon}$ *uniformly on $\overline{\Omega}$,* (2) $|\nabla w^{\varepsilon}|$ *is bounded on $\overline{\Omega}$, and* (3) w^{ε} *satisfies the Dirichlet problem*

$$\nabla \cdot \left(|J|(x) \frac{\nabla w^{\varepsilon}}{\sqrt{\varepsilon^2 + |\nabla w^{\varepsilon}|^2}} \right) \quad \text{in } \Omega,$$
$$w^{\varepsilon} = f \quad \text{on } \partial\Omega.$$

CONJECTURE 2. *Suppose w^{ε} satisfies the conditions of Conjecture* 1 *for every $\varepsilon \in (0, 1]$. Then the sequence $\{w^{\varepsilon}\}$ converges uniformly on $\overline{\Omega}$ to the function of the weighted least gradient*

$$u^* = \operatorname{argmin} \left\{ \int_{\Omega} |J|(x) |\nabla u| dx : u \in W^{1,1}_{+}(\Omega) \cap C(\overline{\Omega}), u = f \text{ on } \partial\Omega \right\}.$$

The proof of these conjectures will be the subject of further work.

Acknowledgment. The idea of introducing the weighted MCF problem as a mathematical model of CDII appeared for the first time during the discussions with Adrian Nachman in the spring 2006.

REFERENCES

[1] L. ALVAREZ, P.-L. LIONS, AND J.-M. MOREL, *Image selective smoothing and edge detection by nonlinear diffusion.* II, SIAM J. Numer. Anal., 29 (1992), pp. 845–866.

[2] G. BAL, *Hybrid inverse problems and internal measurements*, in Inverse Problems and Applications: Inside Out II, MSRI Publ. 60, Cambridge University Press, New York, 2013, pp. 325–364.

[3] M. BENZI AND M. TUMA, *A comparative study of sparse approximate inverse preconditioners*, Appl. Numer. Math., 30 (1999), pp. 305–340.

[4] M. BENZI, *Preconditioning techniques for large linear systems: A survey*, J. Comput. Phys., 182 (2002), pp. 418–477.

[5] J. H. BRAMBLE, B. E. HUBBARD, AND T. VIDAR, *Convergence estimates for essentially positive type discrete Dirichlet problem*, Math. Comp., 23 (1969), pp. 695–709.

[6] Y. G. CHEN, Y. GIGA, AND S. GOTO, *Uniqueness and existence of viscosity solutions of generalized mean curvature flow equations*, J. Differential Geom., 33 (1991), pp. 749–786.

[7] M.G. Crandall, H. Ishi, and P. L. Lions, *User's guide to viscosity solutions of second order partial differential equations*, Bull. Amer. Math. Soc., 27 (1992), pp. 1–67.
[8] L. C. Evans and J. Spruck, *Motion of level sets by mean curvature.* I, J. Differential Geom., 33 (1991), pp. 635–681.
[9] L. C. Evans and J. Spruck, *Motion of level sets by mean curvature.* III, J. Geom. Anal., 2 (1992), pp. 121–150.
[10] L. C. Evans and J. Spruck, *Motion of level sets by mean curvature.* IV, J. Geom. Anal., 5 (1995), pp. 77–114.
[11] D. Gilbarg and N. S. Trudinger, *Elliptic Partial Differential Equations*, 2nd ed., Springer, New York, 2001.
[12] R. Jerrard, A. Moradifam, and A. Nachman, *Existence and uniqueness of minimizers of general least gradient problems*, J. Reine Angew. Math., 734 (2018), pp. 71–97.
[13] B. S. Jovanoviĉ and E. Sűli, *Analysis of Finite Difference Scheme For Linear Partial Differential Equations With Generalized Solutions*, Springer, London, 2014.
[14] A. Handlovičova, K Mikula, and F. Sgallari, *Semi-implicit complimentary volume scheme for solving level set like equations in image processing and curve evolution*, Numer. Math., 23 (2003), pp. 675–695.
[15] J. Kačur and K. Mikula, *Solution of nonlinear diffusion appearing in image processing*, Appl. Numer. Math., 17 (1995), pp. 47–59.
[16] O. A. Ladyzhenskaya, V. A. Solonnikov, and N. N. Uraltseva, *Linear and Qusilinear Equations of Parabolic Type*, AMS, Providence, RI, 1968.
[17] O. A. Ladyzhenskaya, *Solution of the first boundary problem in the large for quasi-linear parabolic equations*, Trudy Moscov. Mat. Obšč., 7 (1958), pp. 149–177 (in Russian).
[18] A. Moradifam, A. Nachman, and A. Timonov, *A convergent algorithm for the hybrid problem of reconstructing conductivity from minimal interior data*, Inverse Problems, 28 (2012), 084003.
[19] A. Moradifam, A. Nachman, and A. Tamasan, *Uniqueness of minimizers of weighted least gradient problems arising in hybrid inverse problems*, Calc. Var. Partial Differential Equations, 57 (2018), 6.
[20] A. Nachman, A. Tamasan, and A. Timonov, *Recovering the conductivity from a single measurement of interior data*, Inverse Problems, 25 (2009), 035014.
[21] A. Nachman, A. Tamasan, and A. Timonov, *Current density impedance imaging*, in Tomography and Inverse Transport Theory, Contemp. Math. 559, AMS, Providence, RI, 2011, pp. 135–149.
[22] A. M. Oberman, *A convergent monotone difference scheme for motion of level sets by mean curvature*, Numer. Math., 99 (2004), pp. 365–379.
[23] V. I. Oliker and N. N. Uraltseva, *Evolution of Nonparametric Surfaces with Speed Depending on Curvature,* III, IMA Preprint 895, University of Minnesota, Minneapolis, 1991.
[24] S.Osher and J. Sethian, *Fronts propagating with curvature-dependent speed: Algorithms based on Hamilton-Jacobi formulations*, J. Comput. Phys., 79 (1988), pp. 12–49.
[25] E. Rothe, *Zweidimensionale parabolishe Randwertaufgaben als Grenzfall eidimensionaler Randwertaufgaben*, Math. Ann., 102 (1930), pp. 650–670.
[26] A. A. Samarskii, *On the convergence and accuracy of homogeneous difference schemes for one-dimensional and multidimensional parabolic equations*, USSR Comp. Math. Math. Phys., 2 (1963), pp. 654–696.
[27] A. A. Samarskii and I. V. Fryazinov, *On finite-difference schemes for solving the Dirichlet problem for an elliptic equation with variable coefficients in an arbitrary region*, USSR Comp. Math. Math. Phys., 11 (1971), pp. 109–139.
[28] A. A. Samarskii, *The Theory of Difference Schemes*, Marcell Decker, New York, 2001.
[29] J. Schauder, *Über lineare elliptische differentialgleichungen zweiter ordnung*, Math. Z, 38 (1934), pp. 257–283.
[30] G. C. Scott, M. L. Joy, R. L. Armstrong, and R. M. Henkelman, *Measurement of nonuniform current density by magnetic resonance*, IEEE Trans. Med. Imag., 10 (1991), pp. 362–374.
[31] J. Sethian, *Numerical algorithms for propagating interfaces: Hamilton-Jacobi equations and conservation laws*, J. Differential Geom., 31 (1990), pp. 131–161.
[32] P. Sternberg and W. P. Ziemer, *Generalized motion by curvature with a Dirichlet condition*, J. Differential Equations, 114 (1994), pp. 580–600.
[33] T. D. Ventzel, *The first boundary problem and the Cauchy problem for quasi-linear parabolic equations with several space variables*, Mat. Sb. (N. S.), 41 (1957), pp. 499–520 (in Russian).
[34] N. J. Walkington, *Algorithms for computing motion by mean curvature*, SIAM J. Numer. Anal., 33 (1996), pp. 2215–2238.